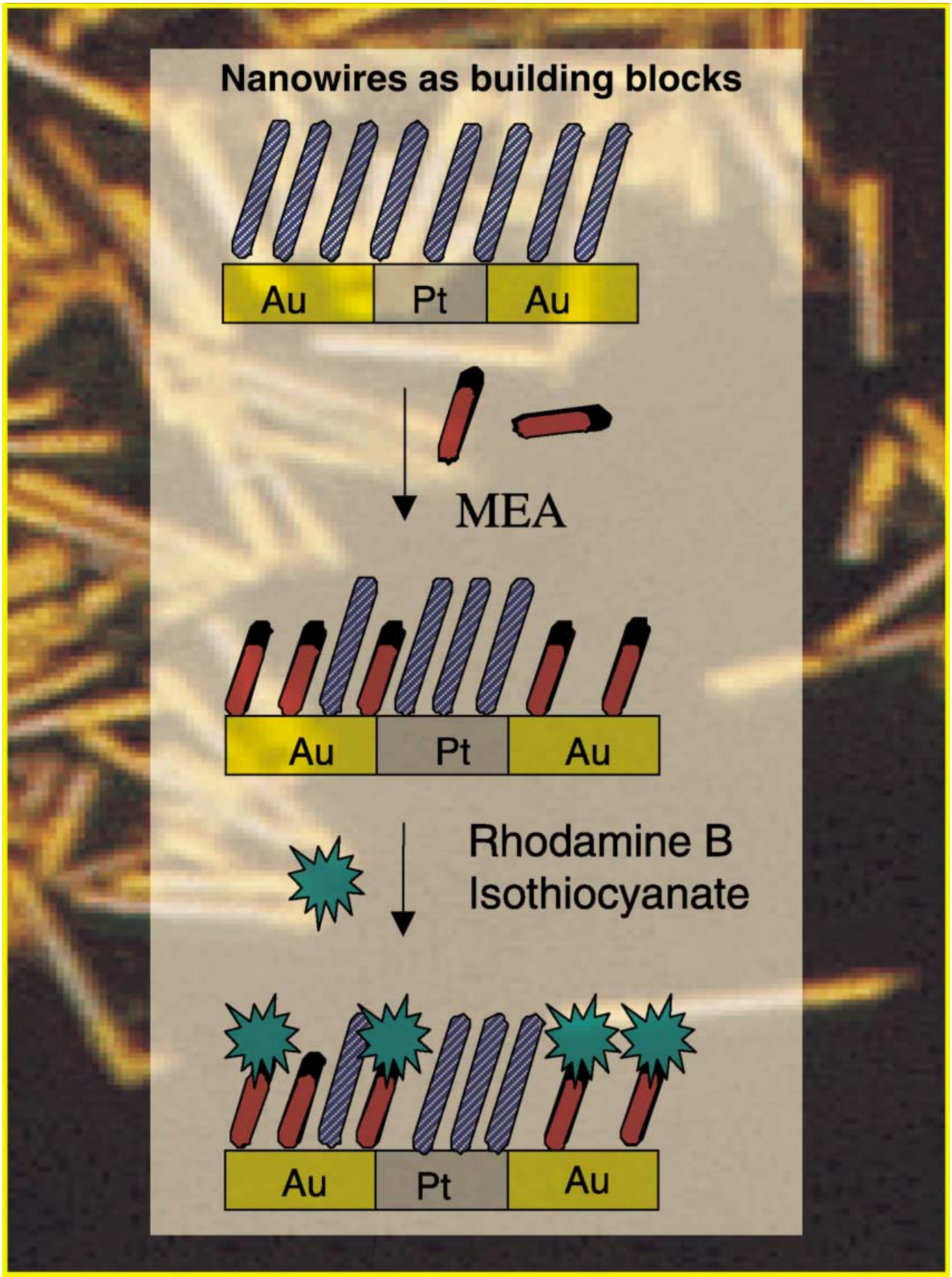

0947-6539/02/0819-4354 $ 20.00+.50/0 *Chem. Eur. J.* **2002**, *8*, No. 19

Nanowires as Building Blocks for Self-Assembling Logic and Memory Circuits

Nina I. Kovtyukhova[a, b] and Thomas E. Mallouk*[a]

Abstract: The concept of assembling electronic circuits from metal nanowires is discussed. These nanowires are synthesised electrochemically by using porous membranes as templates. High aspect ratio wires, which range from 15 to 350 nm in diameter and contain "stripes" of different metals, semiconductors, colloid/polymer multilayers, and self-assembling monolayers have been made by this technique. By using the distinct surface chemistry of different stripes, the nanowires can be selectively derivatized and positioned on patterned surfaces. This allows the current–voltage properties of single and crossed nanowire devices to be measured. Nanowire conductors, rectifiers, switches, and photoconductors have been characterized. Techniques are still being developed for assembling sublithographic scale nanowires into cross-point arrays for memory and logic applications.

Keywords: metal nanowires · nanotechnology · self-assembly · surface chemistry · template synthesis

Introduction

The idea of assembling electronic circuits from molecular-scale devices, which was predicted over 40 years ago in Feynman's visionary "There's plenty of room at the bottom" paper, has recently gained increasing credibility. The steady scaling down of lithographically fabricated devices in silicon integrated circuits has fueled the growth of the enormously successful electronics industry over the last three decades. But, as this technology marches into the nanoscale regime it faces seemingly insurmountable challenges. Complementary metal-oxide semiconductor (CMOS) processes are now approaching physical and practical limits. Thinning of the gate dielectric in field-effect transistors is leading increasingly to unacceptably high tunneling currents. Photolithographic patterning of features below 50 nm will require synchrotrons or other exotic sources such as projection e-beam lithography. Also, the demands of scaling to smaller and faster devices have led (and will continue to lead) to exponential growth in the capital cost of new fabrication facilities. Thus, while it is not clear how it will be done, it is now becoming widely appreciated that the chemical "synthesis" of nanoscale circuits could offer real advantages in terms of both device density and processing cost.[1, 2] This kind of "bottom up" integrated circuit fabrication will rely on the parallel synthesis of large numbers of molecular or nanoscale devices with appropriate electronic functions and their self-assembly into electronic circuits.

Since the first molecular rectifier was proposed by Aviram and Ratner in 1974,[3] tremendous advances have been made in the synthesis, characterization, and assembly of molecule-, polymer- and nanoparticle-based electronic devices.[4–12] Early work by Murray and co-workers described electrochemical rectifiers made of layers of redox polymers.[4] Conducting polymer "transistors", in which changes in the oxidation state of the polymer modulated the conductivity, were reported soon after.[5a] A decade later, the first measurements of electronic device properties in single monolayers of organic molecules began to appear. Unimolecular rectifiers,[7, 8] electronically configurable logic gates,[9] negative differential resistance (NDR) devices,[10] molecular field-effect transistors,[11] and electronically reconfigurable switches[12] have all been fabricated by sandwiching a molecular monolayer between planar (typically micrometer-sized) electrodes.

To exploit the power of these molecules in practical integrated circuits, the issue of defects must be addressed. This is important at two levels. First, one can think of using a self-assembled monolayer (SAM) as a replacement for a device (such as a capacitor or transistor) in a conventional silicon circuit. Because the monolayer contains defects—grain boundaries, steps in the underlying metal contact, dust particles, and the like—processes that give a high yield of robust and reproducible molecular devices are needed. Second, to exploit the power of molecules and nanoparticles at sub-lithographic densities, at least some parts of the circuit must be assembled rather than fabricated in an entirely "top-down" process. Because some defects (such as dislocations in

[a] Prof. T. E. Mallouk, Dr. N. I. Kovtyukhova
Department of Chemistry
The Pennsylvania State University
University Park, PA 16802 (USA)
Fax: (+1) 814-863-8403
E-mail: tom@chem.psu.edu

[b] Dr. N. I. Kovtyukhova
Institute of Surface Chemistry
National Academy of Sciences of the Ukraine
17, General Naumov Str., 03680 Kyiv (Ukraine)

  0947-6539/02/0819-4355 $ 20.00+.50/0

crystals) are inherent in all chemical assembly processes, defect tolerant circuit architectures are needed.

In principle, both problems can be overcome by using molecular junctions between nanowires as device elements, and self-assembled arrays of nanowires as function blocks in larger circuits.[2, 13–15] Figure 1 shows a simple scheme in which nanowires form an array that contains memory or logic elements at the cross points. Because of the extremely small crossing area of cyclindrical nanowires, the likelihood that an individual cross point will coincide with a defect in a SAM device layer is small. Provided that the overall architecture of the circuit is defect-tolerant, such an array could provide memory or logic at densities as high as 10^{11} devices per cm^2. Fabricating useful circuits at higher integration levels turns out to be rather challenging because of geometric and dynamic factors and requires innovative architectural approaches.[1]

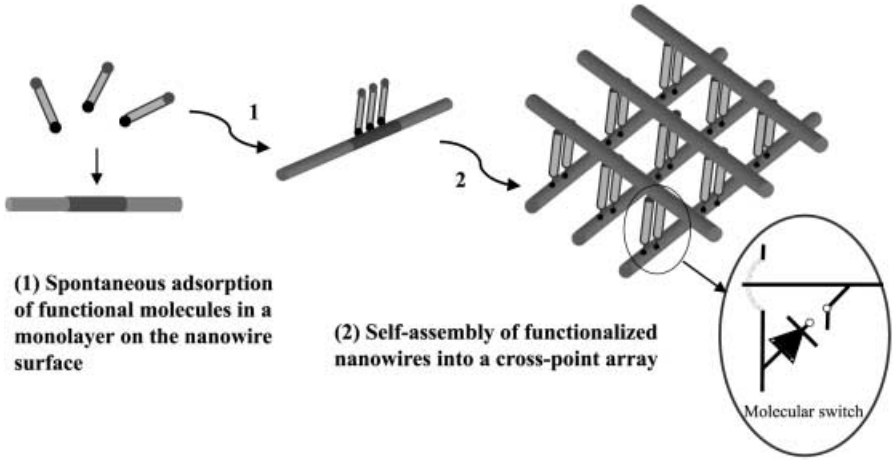

Figure 1. Schematic drawing of the assembly of a two-dimensional cross-point array from metal nanowires and functional molecules. In order for the cross-point array to act as a functional memory or logic device, a configurable switch is needed at each junction. A series diode is also required for device isolation.

Assembly schemes based on fluidic, electrostatic, and/or capillary interactions are candidates for coaxing nanowires to form such imperfect but functional crosspoint arrays. Very recently, the viability of this kind of approach has been impressively demonstrated by the fabrication of logic gate structures from semiconductor nanowires,[13] a reversible bistable carbon nanotube-based memory bit,[14] and logic circuits that contain carbon nanotube transistors.[15] In these examples the nanowires and nanotubes are used as both interconnects and as active devices by exploiting their intrinsic electronic properties. The vapor–liquid–solid growth[16, 17] of nanowire-shaped semiconductor crystals allows one to apply some well-established principles of semiconductor electronics at the low end of nanometer size regime. Recent reports of the microfluidic alignment of semiconductor nanowires in parallel (though not extremely dense) cross-point arrays[18] represent an important milestone in the realization of self-assembling circuits.

A related approach to functional circuits involves the self-assembly of composite nanowires with molecular-scale components embedded within, or grown as coatings on, metals. The advantage offered by metal-based nanowires is that they already provide the requisite control over surface chemistry, length, diameter, and transport properties. Compared with carbon nanotube and semiconductor nanowires, metals can also provide simpler contacting chemistry and lower resistivity, which in principle should translate to faster switching speeds. In the case of carbon nanotubes, reliable control over their length and diameter, electronic properties determined by the carbon helix pitch, and surface chemistry are still formidable challenges. Although carbon nanotubes and related covalent structures are less susceptible to failure by electromigration, this problem is expected to become serious only below about 10 nm diameter with metal wires. Thus metal nanowires could provide an early entry point into self-assembled electronics. In the long term, scaling below 10 nm feature sizes may not be achievable with metals. Thus, the ultimate scaling of electronic circuits to molecular dimensions is likely to require solutions to the problems of synthetic control in covalent wire and/or nanotube structures.

This paper describes a plausible strategy, or better to say the chemical part of a strategy, for fabricating circuits from metal nanowires and nanowire devices. The devices needed for the kind of array illustrated in Figure 1 are bare and/or insulated metal nanowires. A minimal toolkit of in/on-wire switching, rectifying, and logic-restoring devices will be needed, as well as a set of appropriate surface functionalization and fluidic techniques for fabricating the array. In this review we summarize the progress that has been made and the challenges that remain towards achieving this goal.

Synthesis of Metal Nanowires

High aspect ratio metal nanoparticles can be grown in the solution phase, by using a surfactant mixture that provides selective control over growth rates of different crystal faces.[19, 20] Alternatively, they can be prepared either chemically or electrochemically by template-directed methods. The latter involve metal deposition on or inside a preformed nanoscale template. Free-standing metallic nanowires have been prepared by chemical metal plating on the surface of high aspect ratio particles, such as phospholipid tubules,[21] DNA strands,[22] and carbon nanotubes,[23] by opening and filling nanotubes,[24] by decorating atomic step edges of single-crystal surfaces[25] and by electrochemical and electroless plating inside the pores of inorganic or polymeric template membranes.[26–28] Compared to solution and vapor-phase techniques,[29] the membrane replication method fulfills the

0947-6539/02/0819-4356 $ 20.00+.50/0 *Chem. Eur. J.* **2002**, *8*, No. 19

requirements of future electronic applications particularly well because it provides:

- A technologically simple and inexpensive synthesis of a large number ($\approx 10^8 - 10^{11}$ per membrane) of relatively uniform nanowires with precise control over length and diameter.
- The availability of segmented multicomponent nanowires.[30, 31]
- Relatively easy access to molecular device elements embedded within or grown on the surface of nanowires, by exploiting the surface chemistry of both the metal and the pore walls of the membrane.[32–35]
- The possibility of spatial selectivity in the functionalization of a nanowire.[30, 36, 37] This, in principle, allows one to incorporate more than one device element into a single nanowire.

The electrochemical replication of porous membranes, introduced by Moskovitz[26a] and Martin,[26b] involves the evaporation of a metal film on the backside of an alumina or polycarbonate membrane, which is then used as the cathode in an electrochemical cell. The cylindrical pores determine the diameter of the wires, and the charge passed determines the wire length with almost atomic precision. Membranes with pore diameters ranging from about 15 to 350 nm are commercially available, and can be synthesized in the laboratory by anodic treatment of aluminum metal. Free-standing wires are obtained after dissolving the backside metal film and the membrane itself.

By simply alternating the electroplating solutions and controlling the charge passed in each plating step, one can make a well-defined series of segments of metallic (Au, Ag, Pt, Pd, Cu, Ni, Pb, Sn),[30, 31] semimetallic (Bi),[38] or semiconducting (Se, CdSe, CdTe)[31] compositions along the length of the nanowires. Figure 2 shows some examples of free-standing single- and multicomponent nanowires made by this technique.

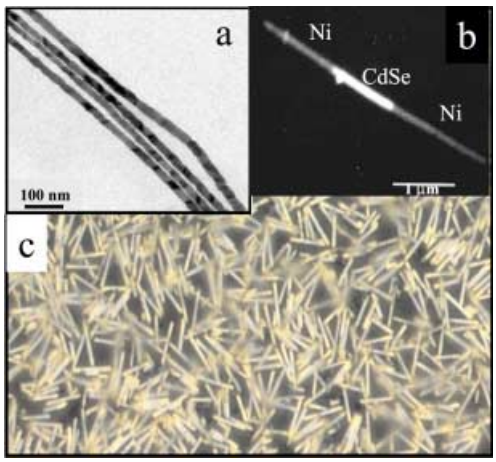

Figure 2. Electron micrographs of a) 20 nm diameter gold wires grown in polycarbonate membranes, and b) a 70 nm diameter Ni-CdSe-Ni wire grown in polycarbonate. An optical micrograph of 350 nm diameter Au-Pt-Au wires is shown in c).

Functionalization and Assembly of Metal Nanowires

Metal nanowires can be derivatized with different kinds of molecules by using well-established methods for preparing self-assembled monolayers (SAMs) and multilayers.[39] For example, 2-mercaptoethanesulfonic acid (MESA) forms a SAM and imparts a pH-independent negative charge to a gold nanowire surface. These anionic nanowires are irreversibly adsorbed from aqueous suspensions onto positively charged surfaces and are highly mobile on negatively charged surfaces.[40] Figure 3 shows how these electrostatic interactions can be used to bind nanowires selectively to substrates with lithographically defined patterns. Anionic MESA-coated gold wires are immobilized as a single-particle thick layer on positively charged (derivatized with 2-mercaptoethylamine (MEA)) gold pads, and can be easily rinsed away from negatively charged SiO_2 areas. On topographically patterned hydrophilic substrates, the hydrophilic anionic nanowires are driven into shallow wells by gravitational forces. With high aspect ratio wells, the wires adopt a parallel orientation because it provides more efficient packing (Figure 3).[40] This

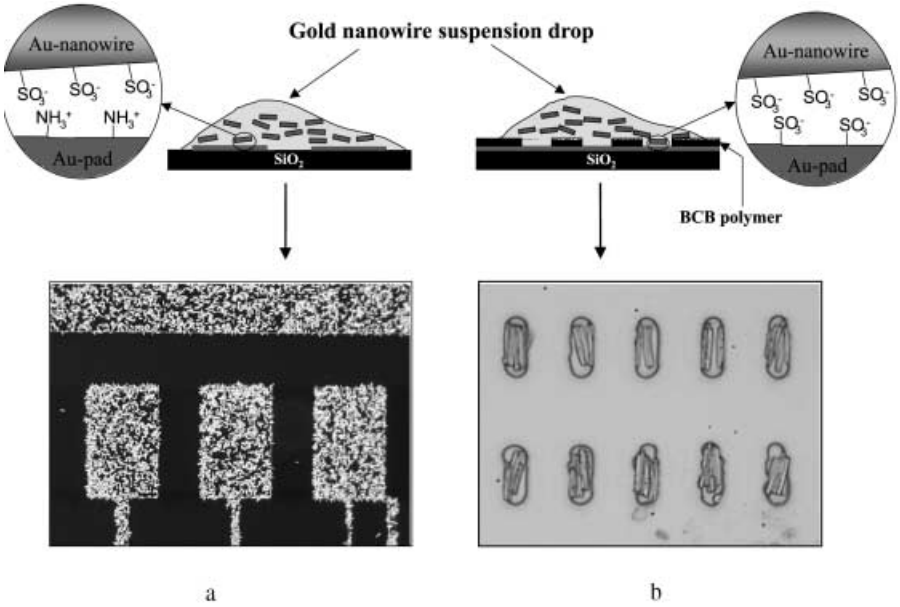

Figure 3. Top: Scheme showing the selective adhesion and alignment of negatively charged gold nanowires on lithographically patterned surfaces. Bottom: a) dark field optical micrograph (500× magnification) of gold nanowires on MEA-derivatized gold pads patterned on a SiO_2/Si-wafer; b) bright field optical micrograph (1000× magnification) of gold wires in oblong wells (4 μm × 8 μm × 600 nm deep) chemically etched in a divinylsiloxanebis(benzocyclobutene) (BCB) polymer layer on Au. The Au metal at the bottom of the wells is derivatized with MESA.

  0947-6539/02/0819-4357 $ 20.00+.50/0

behavior is potentially useful, if it can be better controlled, for making parallel nanowire bundles, each of which represents half of a cross-point array.

More complex anisotropic assembly can be realized if segmented multimetal nanowires are used. Because the segments have distinct surface chemistry, it is possible to achieve spatially selective functionalization along the nanowire length.[30] Figure 4 shows the selective functionalization of an Au/Pt/Au nanowire, based on the differential reactivity of Pt and Au towards thiols and isocyanides, as originally described by Whitesides and Wrighton.[41] A butaneisonitrile monolayer on the Au/Pt/Au wire surface is replaced by a SAM of MEA only on Au, and not on Pt. The MEA-bearing gold portion of the nanowires can be tagged with a fluorescent indicator molecule to image the spatially localized SAMs along the length of the nanowires (Figure 4).

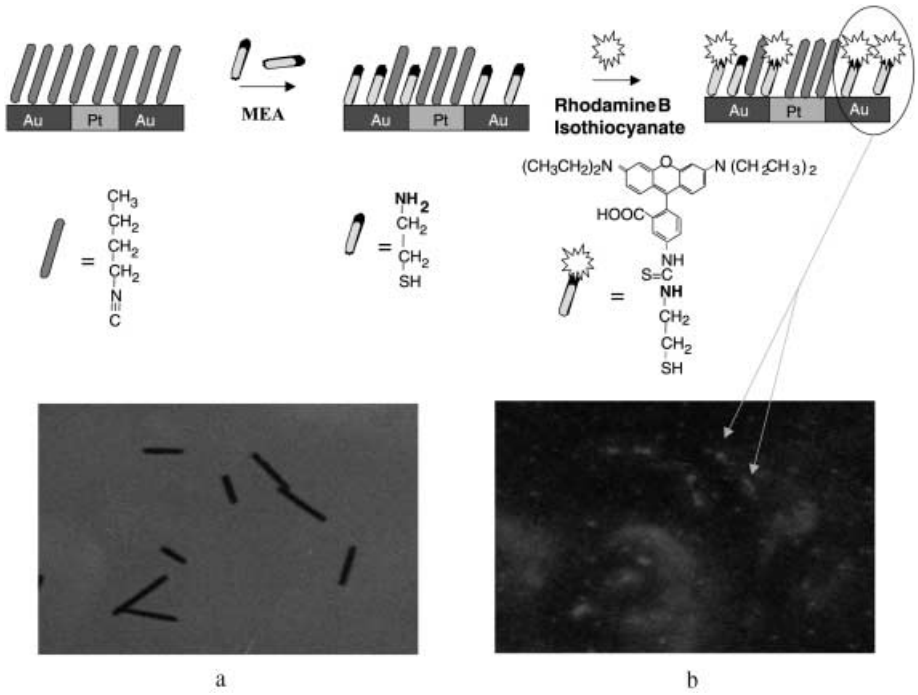

Figure 4. Top: Successive derivatization of Au/Pt/Au nanowires with butaneisonitrile and MEA. To make the MEA-bearing ends distinguishable by fluorescence microscopy, the MEA molecules were coupled with rhodamine B isothiocyanate. Bottom: a) bright field optical micrograph and b) fluorescence micrograph of derivatized Au/Pt/Au nanowires (1000 × magnification).

This orthogonal self-assembly technique gives an entry point into the construction of two- and possibly three-dimensional structures by using attractive and repulsive interactions between functionalized segments of the nanowires. Among the possible linker molecules, deoxyribonucleic acid (DNA) is a particularly interesting candidate because of the selectivity and reversibility of hybridization of complementary single strands (ssDNA). Different sequences are readily available as ssDNA strands of precisely controlled length. They can be modified with a variety of functional groups at their termini, thus enabling rich and varied attachment chemistry. These properties have been used to organize metal and semiconductor nanoparticles into microscopic periodic arrays,[42] micrometer sized rings,[43] and "nanocrystal molecules".[44] In these examples the length of the DNA strands is of the order of the nanoparticle size (1.3 – 15 nm). DNA hybridization provides uniform particle separations within the microscopic aggregates,[42a] and directs the spatial organization of nanocrystal dimers, trimers, and oligomers.[44] Formation of one or several DNA duplexes is enough to realize designed nanoparticle assemblies.

DNA-directed assembly becomes more challenging as the size of the particles increases. In the micrometer regime (as in the case of high aspect ratio nanowires), the roles change, and the particles act as substrates for the ssDNA monolayer, which is supposed to serve as a thin layer of "glue". Appropriate positioning of these large particles requires good hybridization efficiency of multiple complementary strands, and, hence, high quality of the adsorbed ssDNA monolayers. UV-visible and fluorescence spectroscopy show that the adsorption and hybridization behavior of a thiol-modified 36-mer ssDNA on gold nanowires[36] mimics that bound to a planar Au film.[45, 46] This makes DNA adsorption strategies, developed for planar substrates, applicable to the nanowires. The adsorption equilibrium for ssDNA on Au nanowires can be fit to a Langmuir adsorption isotherm, and monolayer coverage is estimated at 5.7×10^{12} molecules per cm^2, or ≈ 0.06 molecules per nm^2; this is comparable to that found on planar substrates.[45, 46] For 36-mer ssDNA, this coverage can be considered the optimum, above which interchain steric effects become pronounced.[46] As in the case of gold films, thiolated DNA strands can adsorb on the nanowires not only through thiol group but also through other polar groups such as nitrogeneous bases. This nonspecific adsorption can be reduced by treatment with mercaptohexanol, thus making the nucleobases more available for hybridization.[46] The use this adsorption scheme with gold nanowires (Figure 5, route 1) allows one to increase the efficiency of hybridization with complementary strands in solution from $21 \pm 3\%$ to $63 \pm 11\%$. A more complex derivatization scheme (shown in Figure 5, route 2) involves successively treating gold nanowires with mercaptohexadecanoic acid (MHDA), bis-aminated polyethylene glycol, 1,4-phenylene diisothiocyanate, and amine-tagged ssDNA. Figure 5 shows the assembly of gold nanowires on the ssDNA-modified surface of lithographically defined gold pads, by using complementary and noncomplementary DNA linking sequences. A coverage of $0.9 – 1.5 \times 10^6$ particles per cm^2 can be achieved by means of complementary

0947-6539/02/0819-4358 $ 20.00+.50/0 *Chem. Eur. J.* **2002**, *8*, No. 19

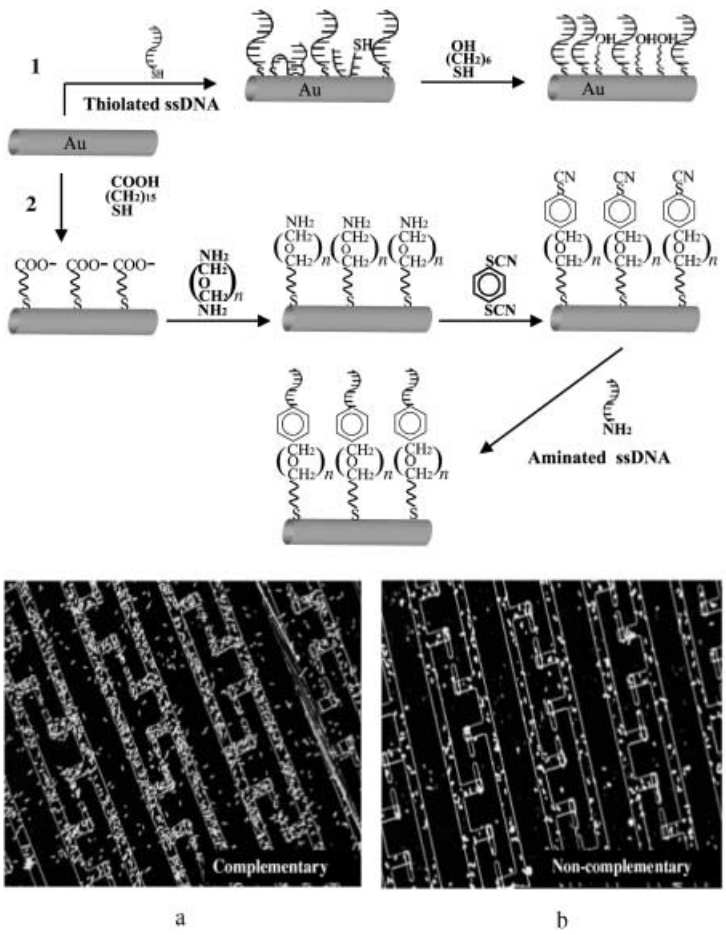

Figure 5. Top: Scheme for successive derivatization of Au nanowires with 1) thiolated ssDNA and mercaptohexanol; 2) mercaptohexadecanoic acid (MHDA), bisamino polyethylene glycol, 1,4-phenylene diisothiocyanate, and amine-tagged ssDNA. Bottom: Dark field optical micrographs (500 × magnification) of gold nanowires derivatized according to the scheme 2 and adsorbed on lithographically patterned surfaces. Gold patterns were prepared on a SiO_2/Si-wafer and derivatized with a) complementary ss DNA and b) noncomplementary ssDNA.

interactions. On the noncomplementary surface, about 25% of this coverage is obtained through nonspecific interactions of surface-bound ssDNA.[36, 37]

By using in-membrane and in-solution derivitization sequences, ssDNA-bearing areas can be precisely localized either at the tips or along the nanowire at any distance from the tips.[36, 37] Within membrane, only tips of a metal nanowire are exposed to DNA molecules. A fluorescence micrograph of nanowires derivatized in this way and then subjected to hybridization with rhodamine-labeled complimentary ssDNA shows that the DNA molecules are bound only at the tips (Figure 6). For spatially selective derivatization along the length of a nanowire, the differential binding of thiols and isonitriles to Au and Pt nanowire segments can be applied to Pt/Au/Pt and Au/Pt/Au/Pt wires. This site-specific functionalization allows one to assemble nanowires into different shapes. For example, crosses, T's, and triangles can be assembled in suspensions in ≈50%, ≈50%, and ≈5% yields, respectively.[37] Control experiments again establish that complementary sequences are required to achieve a high yield of crosses and T's. Further efforts concentrating on improving the hybridization efficiency and avoiding nonspecific wire–wire and wire–surface interactions are necessary to extend this technique to a more deterministic "alphabet soup" of nanowire assemblies.

Fabrication of Nanowire Device Elements

The incorporation of device elements into template-prepared nanowires involves growing thin films of electroactive materials between the nanowire segments or along their length. Wet chemical assembly, which is an inexpensive and technologically simple alternative to vapor-phase deposition methods, is particularly well suited to this application. There are essentially three strategies for controlling such films to nanometer precision: 1) self-assembly of monolayers of organic molecules,[7–12, 39] 2) layer-by-layer assembly of multilayer films from inorganic (semiconductor, metal) nanoparticles and organic molecules (e.g., polymers),[47] and 3) electrochemical plating of polymer and semiconductor films. All three methods have now been used to make "stripes" of active materials within the wires.[31, 33–35] Densely packed SAMs of mercaptohexadecanoic acid (MHDA) can be grown at the exposed tips of gold nanowires through the formation of Au–S bonds[35] (see Figure 7, route 1). Electroless deposition of a thin Au layer on the top of MHDA monolayer is used to avoid short circuits that can form when the top metal layer is grown electrochemically. The fabrication of the in-wire junction by layer-by-layer assembly of a multilayer semiconductor/polymer film is shown schematically in Figure 7, route 2.[33, 34] Cationic TiO_2 nanoparticles and anionic polystyrenesulfonate (PSS) chains spontaneously adsorb in monolayers onto the growing surface, and the film growth is limited in each cycle by inversion of the surface charge. TEM images of the both types of in-wire devices show the presence of the metal/film/metal junction (Figure 7, a, b). Photoconductive CdSe and CdTe can also be grown electrochemically as thin films between gold or nickel nanowire segments.[31]

Two different synthetic sequences can be used to make the on-wire device element, in which a functional film covers the walls of a metal nanowire. The first one relies on the reactivity of the metal wire surface, and involves layer-by-layer growth of organic polyelectrolyte or semiconductor/polymer multilayer films.[32–34] This method can be used with free-standing nanowires, which are suspended in solution by dissolving both the template membrane and the silver backing layer (Figure 8, route 2). Alternatively, a metal nanowire array attached to the silver base, a so-called "brush", can be prepared by dissolving away the membrane and leaving the silver backing untouched. Schematic representations of the brush technique and TEM images of different films that have been grown on metal nanowire walls are shown in Figure 8. To make concentric devices accessible for further functionalizaton at the tips, one can first electroplate sacrificial metal segments on the nanowire ends and dissolve them when the wires are removed from the backing layer.[32]

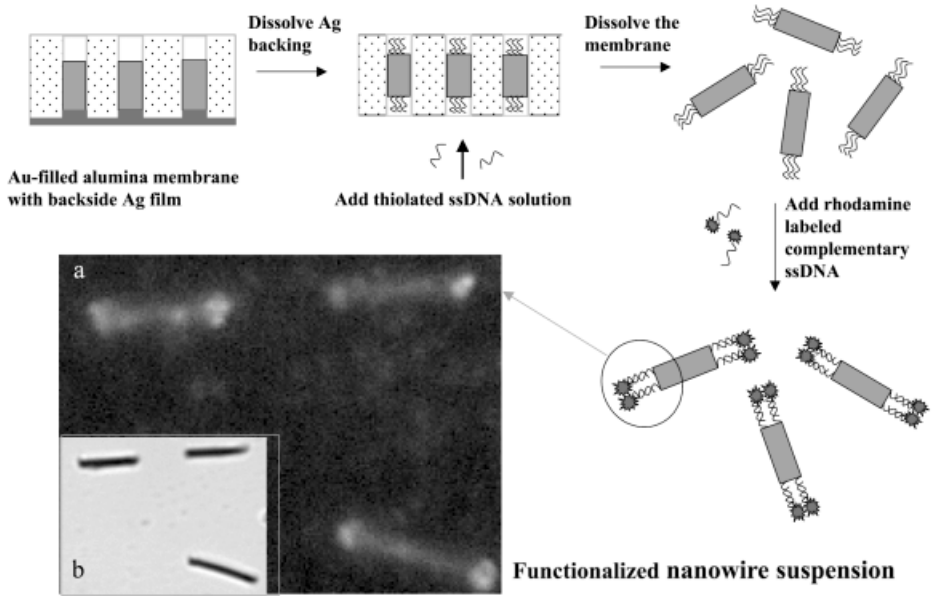

Figure 6. Scheme for in-membrane derivatization of the tips of gold nanowires with thiolated ssDNA. The nanowires are released into solution and then treated with rhodamine-labeled complementary ssDNA, which makes their tips fluorescent. a) Fluorescence and b) bright field micrographs of 350 nm diameter gold wires derivatized according to the scheme.

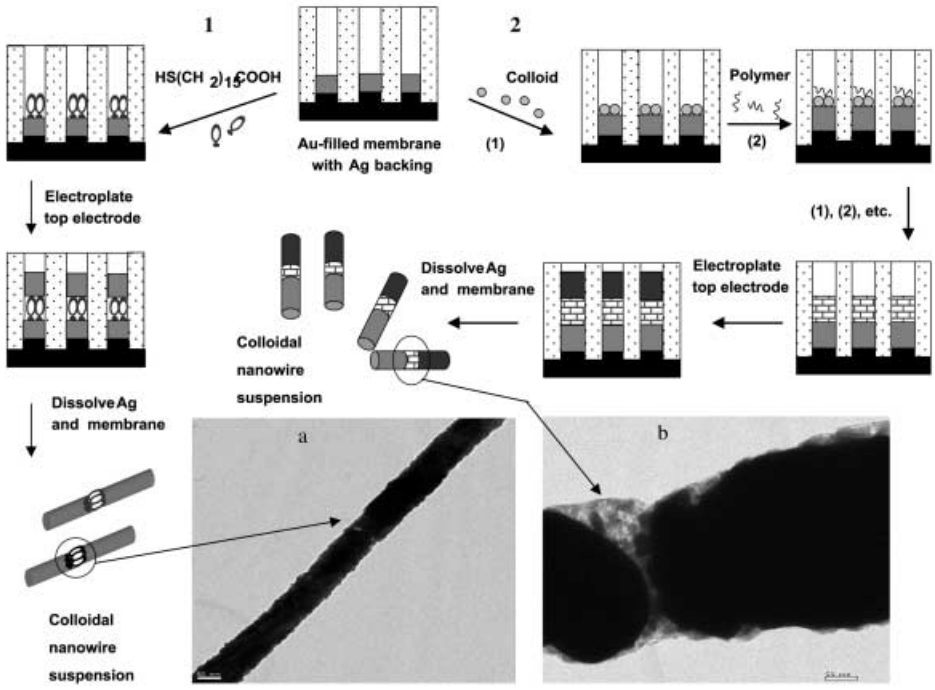

Figure 7. Top: Scheme for preparing in-wire devices by: 1) self-assembly of a MHDA monolayer, or 2) layer-by-layer assembly of TiO_2/PSS multilayer film on the exposed tip of a bottom metal electrode, followed by electroless seeding and electroplating of a top metal electrode. Bottom: TEM images of an as-prepared a) Au/$S(CH_2)_{15}COOH$/Au device, and b) a $Ag(TiO_2/PSS)_9TiO_2$/Au device. In b), electron beam-induced melting of the junction allows one to visualize the junction.

The second reaction sequence exploits surface chemistry of the membrane pore walls. The membrane is first used as a substrate in a conventional layer-by-layer deposition procedure, resulting in semiconductor/polymer tubule shells that are stuck to the walls. The metal nanowire core is then electrochemically or chemically grown inside these shells, as shown schematically in Figure 8, route 1.[33, 34] Figure 8a and b shows TEM images of free-standing, rigid TiO_2/PSS tubules with uniform, densely packed walls and concentric device structures prepared by electrochemically filling the tubules with gold.

Electrical Properties of Template-Grown Nanowire Devices

Nanowire integration into a circuit can be achieved by AC electrofluidic alignment, which positions individual nanowires or nanowire devices between lithographically prepared contact pads[48] (Figure 9, route 1). For a concentric device, the top electrical contact can be made by evaporation of an Ag-stripe at right angles to the wire (Figure 9, route 2), or by fluidic alignment of a second wire that crosses the first.

Electron transport across the monolayer of MHDA molecules in the in-wire Au/MHDA/Au structure occurs by tunneling. The barrier height, the magnitude of the tunneling current, and the breakdown fields for these devices are consistent with previous observations (made by conducting tip AFM and related techniques) of tunneling in SAMs.[49] These devices degrade and eventually become short circuits if the breakdown voltage is repeatedly exceeded, but they are stable if the voltage is kept below this limit.[35]

For the semiconductor/polymer devices, either in-wire or concentric, the room-temperature I-V characteristics show the expected rectifying behavior.[33, 34] In the case of Au-(MEA)/(ZnO/PSS)$_{19}$ZnO/Ag devices, rectification is a result of charge injection at the metal/ZnO/PSS-film interface rather than tunneling (Figure 9a). With $Ag(TiO_2/PSS)_9TiO_2$/Au devices, switching behavior and hysteresis that could not be described by Schottky or Fowler–Nordheim equations was found (Figure 9b). The observation of hysteresis is surprising and potentially interesting in terms of switching or memory

  0947-6539/02/0819-4360 $ 20.00+.50/0 *Chem. Eur. J.* **2002**, *8*, No. 19

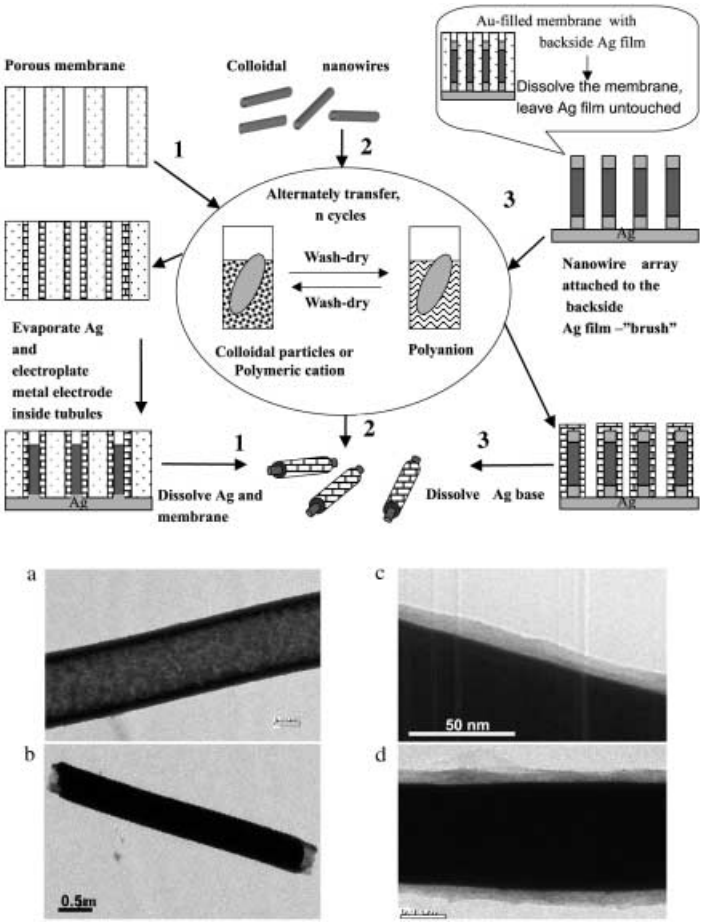

Figure 8. Top: Scheme for preparing on-wire (concentric) devices using layer-by-layer assembly techniques: 1) a multilayer TiO_2/PSS tubule is deposited on the pore walls of an alumina membrane from TiO_2 nanoparticle and PSS solutions (gold nanowires are then electroplated inside the tubules); 2) A ZnO/PSS film multilayer filmis grown on the surface of free-standing gold nanowires by using ZnO nanoparticle and PSS solutions; 3) a multilayer PAH/PSS film is deposited on the surface of an Au/Ag nanowire array attached to a silver base by using polyallylamine and PSS solutions. Bottom: TEM images of a) a free-standing $(TiO_2/PSS)_9TiO_2$ tubule released into solution by dissolving the membrane; b) a Au/$(TiO_2/PSS)_9TiO_2$ concentric device prepared according to route 1; c) a Au/$(PSS/PAH)_{10}$ concentric device prepared according to scheme 3; d) a Au/$(ZnO/PSS)_{19}ZnO$ concentric device prepared according to route 2.

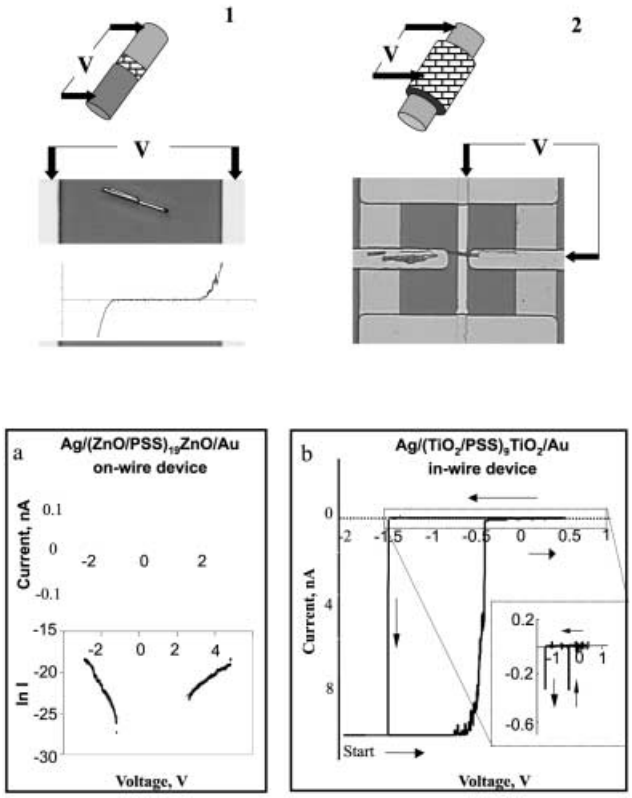

Figure 9. Top: Optical micrographs of test structures for measuring the electrical properties of 1) in-wire devices and 2) on-wire devices in which the semiconductor/polymer film covers the walls of the nanowire. Bottom: a) I-V characteristics of an on-wire Au(MEA)/$(ZnO/PSS)_{19}ZnO$/Ag device (top), the data are plotted in Schottky coordinates (bottom); b) I-V curves for an in-wire Ag$(TiO_2/PSS)_9TiO_2$/Au device showing the hysteresis loop when the scan is reversed at intermediate voltage. The scan shown was initiated at -2.5 V and reversed at $+0.5$ V. The inset curve, with an expanded current scale, shows that the conductance is very low in the reverse sweep.

devices. At present, the reason for this hysteresis is not well understood.

Importantly, the electrical properties of all the in/on-wire devices measured, including both the MHDA SAMs and semiconductor/polymer multilayers, are similar to those of large-area planar devices of the same composition with evaporated top metal contacts. This means that molecular organic and nanoparticle components can be introduced into nanowire devices without qualitative changes in their electrical, and most probably chemical, properties. While the device characteristics shown here are poor by the standards of the semiconductor industry, it is important to note that only primitive layer sequences (simple polymer/colloid repeats) were used. It should be possible to make more structured films in which asymmetry is built in (e.g., with electron- and hole-conducting segments) to allow better rectification ratios, lower turn-on voltages, and more complex device functions.

The possibility of making in-wire junctions with single layers of organic molecules opens the door to testing and using a wider variety of molecular electronic devices in self-assembly circuits.

Some Perspectives on Preparing Molecular Logic-Array Nanoblocks

The possibility of making functional nanowire crosspoint arrays is underscored by results that show the alignment of functionalized nanowires into relatively parallel arrays (Figure 3) and the assembly of small numbers of deliberately functionalized nanowires into deterministic structures (e.g., crosses or T-junctions made by DNA hybridization). If these processes can be better controlled, one could imagine a designed arrangement of cross-point arrays fabricated by joining two wafers, each bearing the appropriately positioned linear rafts of assembled wires. To achieve this, precise alignment of two macroscopic wafers is required. Very recently, high-accuracy alignment of centimeter-sized patterned wafers has been realized by exploiting capillary interactions at the water–air interface.[50] Silica and glass

wafers patterned with millimeter- and micrometer-scale gold features, which were made hydrophobic by adsorbing a SAM of octadecanethiol, were wetted with water on their hydrophilic silica areas and pressed together. Self-alignment of the wafers with an accuracy better than one micrometer results from the minimization of the curvature of the meniscus formed at the water–air interface (Figure 10). The larger

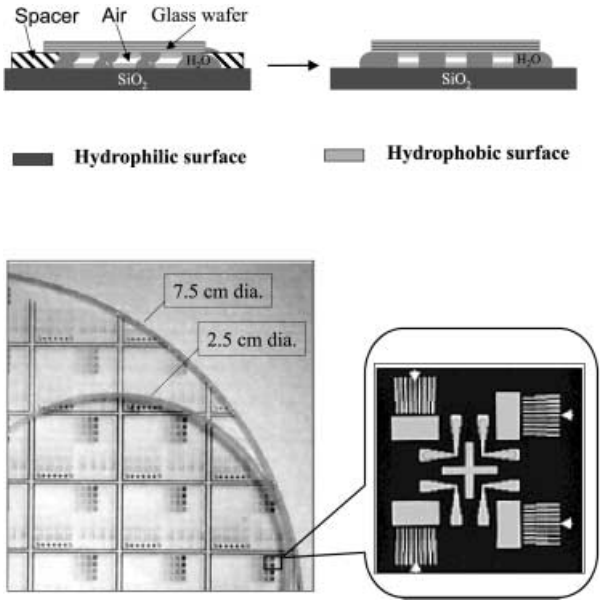

Figure 10. Top: Scheme showing the alignment of planar surfaces using capillary forces. Two silica or glass wafers containing gold features, which were made hydrophobic by adsorbing a SAM of octadecanethiol, are wetted with water on their hydrophilic silica areas and pressed together. Center: An optical micrograph of aligned glass wafers. Bottom: Close up view alignment features used for measurements, which show that the wafers are in alignment to better than one micrometer.

hydrophobic features have been found to direct this alignment, because the micrometer sized patterns are bridged by water and generate no meniscus. Thus, a judicious design of micrometer-sized pads bearing the nanowire "rafts", guided into alignment by macroscopic hydrophobic/hydrophilic boundary areas, could be used to create cross-point array nanostructures.

Conclusion

Although it is too early to say that the light at the end of the tunnel can be clearly seen for nanowire-based computing, some important milestones have been passed, and they help map out the route to this destination. So far we have established that: 1) template synthesis is an experimentally simple and manufacturable route to multicomponent nanowires with well-controlled physical and chemical parameters, 2) site-specific chemical self-assembly directs the assembly of nanowires into surface-bound arrays and designed shapes in solution, 3) nanowire device elements can be made by combining self-assembly with electrochemical and electroless deposition, 4) the availability of in-wire and concentric rectifying films opens up the possibility of constructing logic gates and cross-point devices by means of electrofluidic or chemically driven nanowire assembly, 5) lithographic-scale relief patterns can template the assembly of nanowire arrays with sublithographic pitch, and 6) wafer patterns can be aligned precisely over large areas by patterning hydrophobic and hydrophilic areas. Many challenges remain in terms of synthesizing and characterizing monolayer and multilayer devices, improving the fidelity of the assembly processes, and scaling the devices and nanowire assembly processes to 30 nm diameter and below. If this can be achieved, then the tools for assembling, testing, and optimizing real nanowire circuits will be in hand.

Acknowledgement

This work was supported by DARPA and ONR under contract number ONR-N00014-98-1-0846. We thank our colleagues Theresa Mayer, Thomas Jackson, Christine Keating, Seth Goldstein, and Michael Natan, as well as the students, postdocs, and visitors (Ben Martin, Jeremiah Mbindyo, Brian Reiss, David Peña, Sarah St. Angelo, Jong-Sung Yu, Baharak Razavi, Irena Kratochvilova, Jim Mattzela, Peter Smith, Marco Cabassi, Achim Amma, and Donna Furnanage) who contributed to the work described in this article.

[1] G. Tseng, J. Ellenbogen, *Science* **2001**, *294*, 1293.
[2] S. C. Goldstein, M. Budiu, *Proc. 28th Ann. Int. Symp. Computer Architecture*, **2001**, in press.
[3] A. Aviram, M. A. Ratner, *Chem. Phys. Lett.* **1974**, *29*, 277.
[4] a) H. D. Abruña, P. Denisevich, M. Umana, T. J. Meyer, R. W. Murray, *J. Am. Chem. Soc.* **1981**, *103*, 1; b) P. Denisevich, K. W. Willman, R. W. Murray, *J. Am. Chem. Soc.* **1981**, *103*, 4727.
[5] a) G. P. Kittlesen, H. S. White, M. S. Wrighton, *J. Am. Chem. Soc.* **1985**, *107*, 7373; b) G. P. Kittlesen, M. S. Wrighton, *J. Mol. Electron.* **1986**, *2*, 23; c) R. Friend, J. Burroughes, T. Shimoda, *Phys. World* **1999**, *12*, 35; d) L. S. Roman, M. Berggren, O. Inganas, *Appl. Phys. Lett.* **1999**, *75*, 3557.
[6] A. P. Alivisatos, *MRS Bull.* **1998**, *23*, 2, 18.
[7] R. M. Metzger, B. Chen, U. Hopfner, M. Lakshmikantham, D. Vuillaume, T. Kawai, X. Wu, H. Tachibana, T. Hughes, H. Sakurai, J. Baldwin, C. Hosch, M. Cava, L. Brehmer, G. Ashwell, *J. Am. Chem. Soc.* **1997**, *119*, 10455.
[8] J. C. Ellenbogen, J. C. Love, *Proc. IEEE* **2000**, *88*, 386.
[9] C. P. Collier, E. W. Wong, M. Belohradsky, F. M. Raymo, J. F. Stoddart, P. J. Kuekes, R. S. Williams, J. R. Heath, *Science* **1999**, *285*, 391
[10] J. Chen, M. A. Reed, A. M. Rawlett, J. M. Tour, *Science* 1**999**, *286*, 1550.
[11] J. Schön, H. Meng, Z. Bao, *Nature* **2001**, *413*, 713
[12] C. P. Collier, G. Mattersteig, E. W. Wong, Y. Luo, K. Beverly, J. Sampaio, F. Raymo, J. F. Stoddart, J. R. Heath, *Science* **2000**, *289*, 1172.
[13] Y. Huang, X. Duan, Y. Cui, L. Lauhon, K. Kim, C. M. Lieber, *Science* **2001**, *294*, 1313.
[14] T. Rueckes, K. Kim, E. Joselevich, G. Tseng, C.-L. Cheung, C. M. Lieber, *Science* **2000**, *289*, 94.
[15] A. Bachtold,P. Hadley, T. Nakanishi, C. Dekker, *Science* **2001**, *294*, 1317.
[16] a) R. S. Wagner,W. S. Ellis, *Appl. Phys. Lett.* **1965**, *4*, 89; E. I. Givargizov, *J. Chem. Phys.* **1975**, 31, 20.
[17] S. W. Chung, J. Yu, J. R. Heath, *Appl. Phys. Lett.* **2000**, *76*, 2068.
[18] Y. Huang, X. Duan, Q. Wei, C. M. Lieber, *Science* **2001**, *291*, 630.
[19] V. Puntes, K. Krishnan, P. Alivisatos, *Science* **2001**, *291*, 2115.
[20] Y. Yu, S. Chang, C. Lee, C. Wang, *J. Phys. Chem. B* **1997**, *101*, 6661.
[21] G. Schnur, R. Price, P. Schoen, P. Yager, *Thin Solid Films* **1987**, *152*, 181.

  0947-6539/02/0819-4362 $ 20.00+.50/0 *Chem. Eur. J.* **2002**, *8*, No. 19

[22] E. Braun, Y. Eichen,U. Sivan,G. Ben-Yoseph, *Nature* **1998**, *391*, 775.
[23] R. Yu, L. Chen, Q. Liu, J. Lin, K. Tan, S. Ng, H. Chan, G. Xu, T. Hor, *Chem. Mater.* **1998**, *10*, 718.
[24] M. Terrones, N. Grobert, W. Hsu, Y. Zhu,W. Hu, H. Terrones, J. Hare, H. Kroto, D. Walton, *MRS Bull*. **1999**, 44.
[25] M. Zach, K. Ng, R. Penner, *Science* **2000**, *290*, 2120.
[26] a) D. Al-Mawlawi, C. Z. Liu, M. Moskovits, *J. Mater. Res.* **1994**, *9*, 1014; b) M. Nishizava, V. P. Menon, C. R. Martin, *Science* **1995**, *268*, 700; c) V. Menon, C. R. Martin, *Anal. Chem.* **1995**, *67*, 1920; d) C. R. Martin, *Chem. Mater.* **1996**, *8*, 1739; e) L. Wang, K. Yu-Zhang, A. Metrot, P. Bonhomme, M. Troyon, *Thin Solid Films* **1996**, *288*, 86; f) C. R. Martin, R. V. Parthasarathy, *Adv. Mater.* **1995**, *7*, 487; g) B. B. Lakshmi, P. K. Dorhout, C. R. Martin, *Chem. Mater.* **1997**, *9*, 857.
[27] Y. Han, J. Kim, G. Stucky, *Chem. Mater.* **2000**, *12*, 2068.
[28] T. Thurn-Albrecht, J. Schotter, G. Kastle, N. Emley, T. Shibauchi, L. Krusin-Elbaum, K. Guarini, C. Black, M. Tuominen, T. Russell, *Science*. **2000**, *290*, 2126.
[29] Y. Kondo, K. Takayanagi, *Science* **2000**, *289*, 606.
[30] B. R. Martin, D. J. Dermody, B. D. Reiss, M. Fang, L. A. Lyon, M. J. Natan, T. E. Mallouk, *Adv. Mater.* **1999**, *11*, 1021.
[31] D. Pena, B. Razavi, P. A. Smith, J. K. N. Mbindyo, M. J. Natan, T. S. Mayer, T. E. Mallouk, C. D. Keating, *Mater. Res. Soc. Symp. Proc.* **2001**, *636*, D4.6.1.
[32] J. S. Yu, J. Y. Kim, S. Lee, J. K. N. Mbindyo, B. R. Martin, T. E. Mallouk, *Chem. Commun*. **2000**, 2445.
[33] N. I. Kovtyukhova, B. R. Martin, J. K. N. Mbindyo, P. A. Smith, B. Razavi, T. S. Mayer, T. E. Mallouk, *J. Phys. Chem. B* **2001**, *105*, 8762–8769.
[34] N. I. Kovtyukhova, B. R. Martin, J. K. N. Mbindyo, T. E. Mallouk, M. Cabassi, T. S. Mayer, *Mater. Sci. Eng. C* **2002**, *19*, 255.
[35] J. K. N. Mbindyo, T. E. Mallouk, I. Kratochvilova, B. Razavi, T. S. Mayer, T. N. Jackson, J. B Mattzela, *J. Am. Chem. Soc*. **2002**, *124*, 4020.
[36] J. K. N. Mbindyo, B. D. Reiss, B. R. Martin, C. D. Keating, M. J. Natan, T. E. Mallouk, *Adv. Mater.* **2001**, *13*, 249.
[37] B. D. Reiss, J. N. K. Mbindyo, B. R. Martin, S. R. Nicewarner, T. E. Mallouk, M. J. Natan, C. D. Keating, *Mater. Res. Soc. Symp. Proc.* **2001**, *635*, C6.2.1.
[38] A. Amma, T. E. Mallouk, unpublished results.
[39] A. Ulman, *Chem. Rev.* **1996**, *96*, 1533.
[40] B. R. Martin, S. St. Angelo, T. E. Mallouk, *Adv. Funct. Mater*. in press.
[41] J. Hickman,P. Laibinis, D. Auerbach, C. Zou, T. Gardner, G. Whitesides, M. Wrighton, *Langmuir* **1992**, *8*, 357.
[42] a) C. A. Mirkin, R. L. Letsinger,R. C. Mucic, J. J. Storhoff, *Nature* **1996**, *382*, 607; b) G. P. Mitchell, C. A. Mirkin, R. L. Letsinger, *J. Am. Chem. Soc*. **1999**, *121*, 8122.
[43] J. Coffer, S. Bigham, X. Li, R. Pinizzotto, Y. Rho, R. Pirtle, I. Pirtle, *Appl. Phys. Lett*. **1996**, *69*, 3851.
[44] a) A. P. Alivisatos, K. P. Johnsson, X. Peng, T. Wilson, C. Loweth, M. Bruchez, Jr., P. Schultz, *Nature* **1996**, *382*, 609; b) C. Loweth, W. Caldwell, X. Peng, A. P. Alivisatos, P. Schultz, *Angew. Chem.* **1999**, *111*, 1925; *Angew. Chem. Int. Ed.* **1999**, *38*, 1808.
[45] R. Georgiadis, K. Peterlinz, A. W. Peterson, *J. Am. Chem. Soc*. **2000**, *122*, 3166.
[46] R. Levicky, T. Herne, M. Tarlov, *J. Am. Chem. Soc*. **1998**,*120*, 9787.
[47] a) D. Feldheim, K. Grabar, M. Natan, T. Mallouk, *J. Am. Chem. Soc.* **1996**, *118*, 7640; b) T. Cassagneau, T. Mallouk, J. Fendler, *J. Am. Chem. Soc.* **1998**, 120, 7848; c) M. Gao, B. Richter, S. Kirstein, H. Mohwald, *J. Phys. Chem*. **1998**, *102*, 4096; d) T. Cassagneau, J. Fendler, T. Mallouk, *Langmuir* **2000**, *16*, 241; e) N. Kovtyukhova, A. Gorchinskiy, C. Waraksa, *Mater. Sci. Eng. B* **2000**, *69–70*, 424.
[48] P. A. Smith, C. D. Nordquist, T. N. Jackson, T. S. Mayer, B. R. Martin, J. Mbindyo, T. E. Mallouk, *Appl. Phys. Lett.* **2000**, *77*, 1399.
[49] D. J. Wold, C. D. Frisbie, *J. Am. Chem. Soc.* **2001**, *123*, 5549.
[50] B. R. Martin, D. C. Furnange, T. N. Jackson, T. E. Mallouk, T. S. Mayer, *Adv. Funct. Mater*. **2001**, *11*, 381.

  0947-6539/02/0819-4363 $ 20.00+.50/0